Parallel genetic adaptation of *Bacillus subtilis* to different plant species

Guohai Hu[1,2,3,6], Yue Wang[1,2,4,6], Christopher Blake[3], Mathilde Nordgaard[3], Xin Liu[1,2,4], Bo Wang[1,2,5,*], Ákos T. Kovács[3,7*]

[1] China National GeneBank, BGI-Shenzhen, 518120 Shenzhen, China

[2] BGI-Shenzhen, 518083 Shenzhen, China

[3] Bacterial Interactions and Evolution Group, DTU Bioengineering, Technical University of Denmark, 2800 Lyngby, Denmark

[4] BGI-Beijing, Beijing, 102601, China

[5] Shenzhen Key Laboratory of Environmental Microbial Genomics and Application, BGI-Shenzhen, 518083 Shenzhen, China

[6] These authors contributed equally

[7] New position: Institute of Biology, Leiden University, 2333BE Leiden, The Netherlands

[*]Corresponding authors: a.t.kovacs@biology.leidenuniv.nl (Ákos T. Kovács), wangbo@cngb.org (Bo Wang)

Abstract

Plant growth-promoting rhizobacteria are known to benefit plants by stimulating their growth or protecting them against phytopathogens. Rhizobacteria must colonize and persist on plant roots effectively to exert their benefits. However, little is known regarding the process of rhizobacteria adapting to different plant species or in alternating host regime in long-term. Here we used experimental evolution and whole-population WGS sequencing to analysis how *Bacillus subtilis* evolves on *Arabidopsis thaliana* and tomato seedlings, as well as in an alternating host regime of the two plants in a static hydroponic setup. We identified parallel evolution across multiple levels of biological organization in all conditions, and highest in two heterogeneous, multi-resource spatially structured environments in gene level. Species-specific adaptation in genetic level was also observed, possibly caused by the selection stress imposed by different host plants. Further, the trade-off between motility and biofilm development was supported by the mutational changes in motility- and biofilm-related genes. Finally, we identified several condition-specific and common targeted genes in different environments by comparing three different *B. subtilis* biofilm adaptation settings. These results demonstrate a common strategy used by *B. subtilis* when adapting to the plant rhizosphere in similar conditions and also reveal the differences of genetic mechanism between the two different host plants, both will likely support strain improvements for sustainable agriculture.

Key words: adaptation, experimental evolution, plant-bacteria interaction, trade-off

Importance

To exert the benefits of rhizobacteria on plant growth and protection against phytopathogens, bacteria must colonize and persist on plant roots effectively. Understanding how rhizobacteria adapt to different plants species will assist strain development in sustainable agriculture. To explore the rhizobacterial adaptation process to different plant species or in alternating host regimes, *B. subtilis* was experimentally evolved on *A. thaliana* or tomato roots, or alternating these plants. Both parallel and species-specific adaptation is revealed at genetic level. Further, the trade-off between motility and biofilm formation was explored. Our results reveal several condition-specific and commonly targeted genes from our experiments and those performed previously with experimentally evolving *B. subtilis* biofilms.

Introduction

In natural environments, plant growth and yield depend on a plethora of interactions within the complex and dynamic communities of bacteria and fungi (Schmidt et al. 2016). The rhizosphere plays an important niche for the mutualistic relationships between plants and the microorganisms in the surrounding soil. Overall, plants exude up to 20% of fixed carbon and 15% of nitrogen into their environment (Haichar et al. 2016; Venturi & Keel 2016), and these exudates shape the microbiome. Importantly, the amount and composition of exudates vary depending on the plant species, the stage of development, and the environmental stresses (Sasse et al. 2018). The exudates contribute a rhizobiome formation by recruiting plant-growth-promoting rhizobacterium (PGPR) and serving as nutrients (Lareen et al. 2016), while PGPRs benefit plant growth and enhance plant tolerance to different abiotic and biotic stresses(Vives-Peris et al. 2020). *Bacillus subtilis* is a soil-dwelling, biofilm forming, Gram-positive PGPR that is commonly found in association with plants and their rhizosphere (Arnaouteli et al. 2021). It has been widely recognized that this bacterial species aids plants in several direct and indirect ways(Blake, et al. 2021). Some *B. subtilis* strains have been applied as biocontrol agents within agriculture, but the effects vary immensely under field conditions (Peng et al. 2011; Wei et al. 2016). To exert their beneficial effects, PGPR usually must colonize and persist on the root surface efficiently, which mainly depends on their ability to form biofilms.

Each plant species has a distinct effect on its rhizobiome that is partly driven by plant-secreted exudates. Root exudates not only provide nutritional source for soil microorganisms, but also serve as a signal to attract or repel specific groups of microbes (Badri et al. 2009). For

22 example, diverse sugars and organic acids induce biofilm formation of *B. subtilis in vitro* or
23 directly on the plant via different molecular mechanisms. Spo0A is a central transcriptional
24 regulator in *B. subtilis* involved in biofilm development (Hamon & Lazazzera 2001). Biofilm
25 formation is triggered when moderate level of phosphorylated Spo0A (Spo0A-P) is established
26 within a cell. The level of Spo0A-P is controlled by five histidine kinases (KinA-E), which
27 respond to different environmental signals (Jiang et al. 2000). Chen et al. described *B. subtilis*
28 biofilm formation on tomato roots to be dependent on KinD and small signaling molecules,
29 possibly L-malic acid, released by the roots to stimulate *B. subtilis* biofilm *in vitro* (Chen, Cao,
30 et al. 2012). In contrast to the observation with tomato, deletion of *kinCD* has only a moderate
31 effect on biofilm formation on *Arabidopsis thaliana* roots (Beauregard et al. 2013), suggesting
32 that the kinase requirement of *B. subtilis* for root colonization differs from one plant to another.
33 In the case of *A. thaliana*, biofilm formation by *B. subtilis* is triggered by plant polysaccharides
34 pectin, arabinogalactan, and xylan, which act both as environmental cues and substrates for
35 matrix synthesis (Beauregard et al. 2013). Moreover, the disaccharide sucrose that is abundantly
36 secreted from plant roots, activates a signaling cascade to trigger solid surface motility and
37 promotes rhizosphere colonization by *B. subtilis* (Tian et al. 2021).

38 Interestingly, a *B. subtilis* strain isolated from the banana rhizosphere and a *Bacillus*
39 *amylolicefaciens* strain isolated from the cucumber rhizosphere colonize their original plant
40 hosts more efficiently than the non-host plant (Zhang et al. 2014), demonstrating a species-
41 specific colonization pattern. Additionally, organic acids detected exclusively in one of the plant
42 species induce the chemotaxis and biofilm formation of the corresponding bacterial isolate from

43 that given host (Zhang et al. 2014). Chemotaxis and swarming motility are important for plant
44 colonization (Zhang et al. 2014; Gao et al. 2016). Defect in chemotaxis or swarming reduce the
45 ability of *B. subtilis* to efficiently colonize tomato seedlings in a gnotobiotic system (Gao et al.
46 2016). Similarly, mutants lacking flagellum production are unable to colonize the roots of *A.*
47 *thaliana* in a static hydroponic setup and tomato in a gnotobiotic system (Allard-Massicotte et
48 al. 2016; Gao et al. 2016). In addition to testing specific mutants, experimental evolution
49 provides a powerful tool to reveal the molecular mechanisms related to interaction with a plant,
50 as microbes adapt to the plant root niche (Lenski 2017). Experimentally evolved clones of
51 *Bacillus thuringiensis* from *A. thaliana* roots displayed improved root colonization ability and
52 enhanced swarming, while those were impaired in swimming, in addition to altered bacterial
53 differentiation and pathogenicity (Lin et al. 2021). In a similar setup, when *B. subtilis* was
54 adapted to *A. thaliana* roots, evolved isolates demonstrated elevated root colonization and
55 impaired swimming and swarming motility (Nordgaard et al. 2022), indicating a possible
56 biofilm-motility trade-off. *Pseudomonas protegens*, adapted to *A. thaliana* rhizosphere in an
57 axenic sandy condition, exhibited enhanced swimming motility and impaired swarming
58 motility (Erqin Li et al. 2021). These results all highlight the existence of an evolutionary trade-
59 off between biofilm development and motility. However, it remains largely unknown how such
60 mechanisms supervene from an evolutionary perspective.

61 Since crop rotation regime has great influence on soil multifunctionality and bacterial
62 community in agroecosystems (Minghui Li et al. 2021), we asked whether a plant colonizing
63 bacterium adapts differently in an alternating host regime compared with using the same plant

64 throughout the experiment. In addition, we questioned what portion of bacterial adaptation on
65 a plant root will be host specific. To explore these questions, we employed experimental
66 evolution combined with whole-population metagenome sequencing method to analyze how *B.*
67 *subtilis* evolves on *A. thaliana* and tomato seedlings, as well as in an alternating host regime of
68 these two species in a static hydroponic setup. We identified parallel evolution across multiple
69 levels of biological organization and a higher gene-level parallelism in populations evolved in
70 an alternating host regime. We also observed species-specific adaptation at genetic level, which
71 was potentially provoked by specific host plant-imposed selection, either due to root exudates,
72 plant polysaccharides, or certain stress conditions. Additionally, motility-biofilm trade-off was
73 revealed in the mutational landscape of related genes, in addition to reduced swimming and
74 swarming motility. Finally, we identified several condition-specific and shared list of mutated
75 genes of *B. subtilis* when evolved in different biofilm environments.

76 # Results

77 **B. subtilis *shows rapid improvement and diversification during evolution on plant roots***

78 Do plant colonizing bacteria adapt differently in an alternating host regime compared with a
79 setup where the same plant is used throughout the experiment? To investigate this, we tested
80 adaptation of *B. subtilis* to the roots of two different plant species and compared those with a
81 condition where plants were sequentially alternated. Therefore, starting from a clonal *B. subtilis*
82 DK1042 strain, four different evolution experiments each with five parallel lineages (from A to
83 E), were passaged on both *A. thaliana* and tomato seedlings for 20 transfers, spanning over a
84 total of 40 days (**Fig. 1a,** and **1b**). We conducted two mono-host evolution experiments, one
85 using only ***A***. *thaliana* (Bs_root_**A**) and another with **T**omato (Bs_root_**T**), as well as two host-
86 cycling evolution experiments, which either started on ***A***. *thaliana* (Bs_root_**A**T) or **T**omato
87 (Bs_root_**T**A) and switched the plant species after every third transfers. Evolved clones from
88 Bs_root_A setup have been examined in details previously (Blake, et al. 2021). To evaluate the
89 improvements in root colonization during the experimental evolution, colony forming unit
90 (CFU) per gram of roots was measured after transfer 1, 5, 10, 17, and 20 (T1, T5, T10, T17,
91 and T20 respectively). As expected (Blake, et al. 2021; Lin et al. 2021; Nordgaard et al. 2022),
92 root colonization ability improved significantly in all evolving lineages and conditions, on
93 average 9.10-fold, 7.41-fold, 25.29-fold, and 11.98-fold after 20 transfers in Bs_root_A,
94 Bs_root_T, Bs_root_AT, and Bs_root_TA, respectively (**Fig. 1c**). Furthermore, morphological
95 diversification was also observed in all evolving lineages and conditions in the CFU assays with
96 morphotypes termed as Wrinkle (WR), Snow (SN) and Smooth (SM) (Blake, Nordgaard, et al.

97 2021), where colony morphology of WR variant was comparable with the ancestor. To
98 investigate how the distribution of the distinct morphotypes developed during the experimental
99 evolution, overnight-grown cultures of the frozen stocks of evolved populations from root 5,
100 10, 17 and 20 as well as from the ancestral strain ("transfer 0") were prepared and plated on
101 LB-agar. Different morphological variants were identified and counted to calculate the ratio of
102 a given morphotype at each time point for each lineage. In all four conditions, WR was the most
103 abundant in all lineages through the experiment (**Fig. 1d**). SN appeared in all lineages at T5
104 reaching an average frequency of 21.78%, 15.48%, 23.81%, and 21.28% in Bs_root_A,
105 Bs_root_T, Bs_root_AT, and Bs_root_TA, respectively (**Fig. 1d**), however was below detection
106 limit in some of the lineages at T10 and T17, and raised again in all lineages at T20. SM was
107 observable in 11 of the 20 lineages at T10 and only absent in one lineage at T17 and T20 (**Fig.**
108 **1d**). The three distinct morphotypes coexisted until the end of the evolution experiment,
109 reaching on average highly similar ratios of approximately 80% WR, 17% SN and 3% SM in
110 all four evolution experiments, which showed astounding degree of parallelism at morphotypic
111 level.

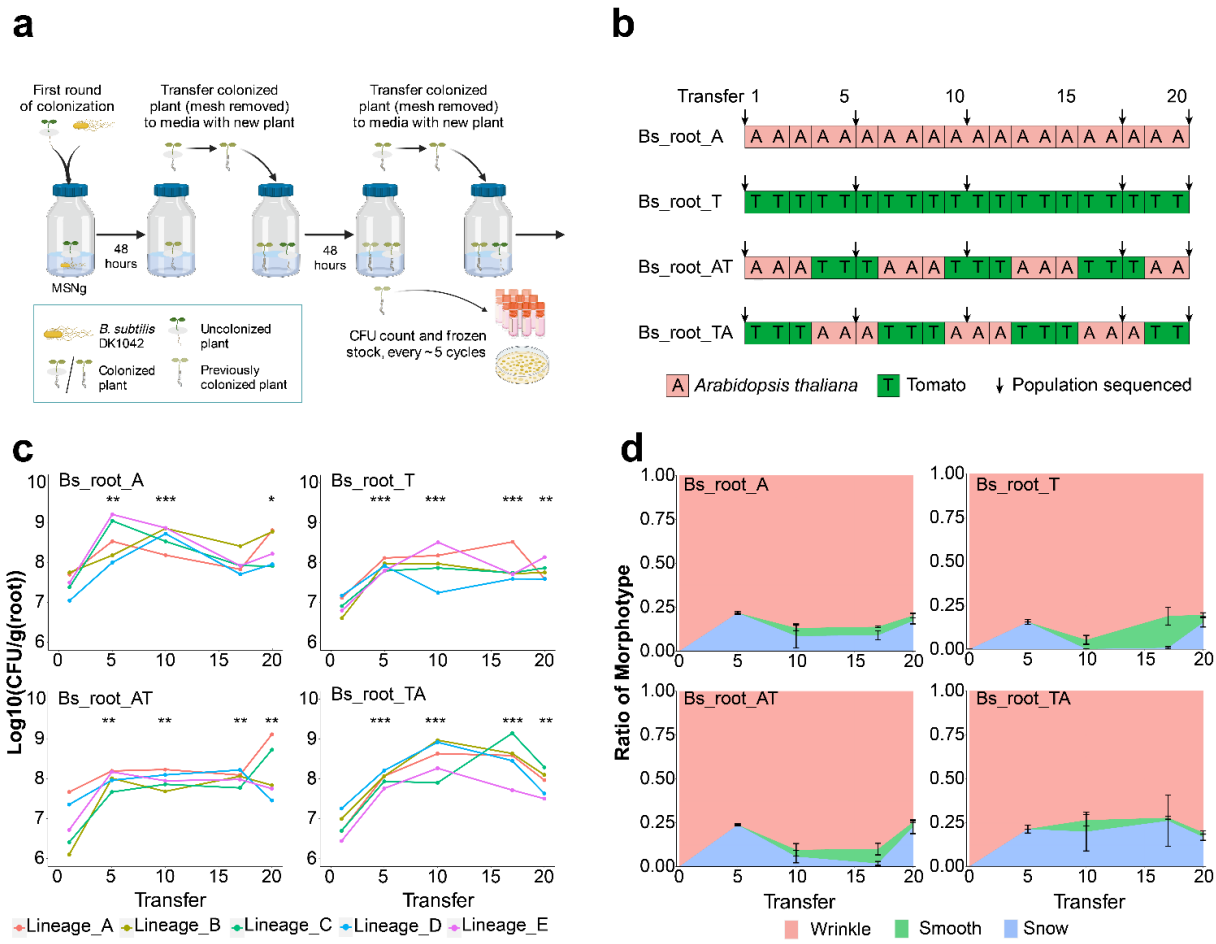

Fig. 1 Evolution of *B. subtilis* on different plant roots. a. Experimental evolution scheme of *B. subtilis* adapting to plant seedling (Created with BioRender.com), **b.** In total four evolution experiments were conducted, either as mono evolution experiments, with only *A. thaliana* or tomato seedlings, or cycling evolution experiments, where the plant species was switched after every third transfer. Sequenced population samples are indicated with an arrow. **c.** root colonization ability was detected during the experiment as CFU per gram root for T1, T5, T10, T17, and T20 in all lineages. (*: $P < 0.05$, **: $P < 0.01$, ***: $P < 0.001$). **d.** the dynamic frequency changes of different morphotypes along the evolution experiment in average of all five populations in each condition (n = 5), data represent mean and error bars represent standard error.

123

124 ***Evolved isolates showed impaired motility***

125 In a soil environment, bacterial cells need to actively move towards the plant roots during the
126 initial phase of root colonization, as well as when recolonizing (Allard-Massicotte et al. 2016).
127 We hypothesized that, in the static hydroponic setup, which select for a regular root
128 recolonization, including chemotaxis, biofilm formation and dispersal, the motility would
129 improve significantly during the evolution experiment, resulting in better root colonization. To
130 examine this, evolved end-point isolates from Bs_root_A and Bs_root_T were tested for
131 swimming and swarming motility, by spotting 2µL of an overnight culture on 0.3% and 0.7%
132 LB-agar, respectively. Contrary to our expectations, none of the tested seven isolates evolved
133 on *A. thaliana*, as well as none of the tested five isolates evolved on tomato, showed
134 improvements in either swimming or swarming (**Fig. 2**). Instead, most isolates displayed
135 significantly smaller swimming radius after 6h and 8h compared with the ancestor, although all
136 isolates colonized the entire plate after 24h, thus mobility was preserved. Importantly, other
137 form of motility, e.g. sliding (Kovács et al. 2017; Hölscher & Kovács 2017), might mask the
138 effect of swimming after 24h. Moreover, all isolates exhibited either delayed, reduced or even
139 impaired swarming abilities.

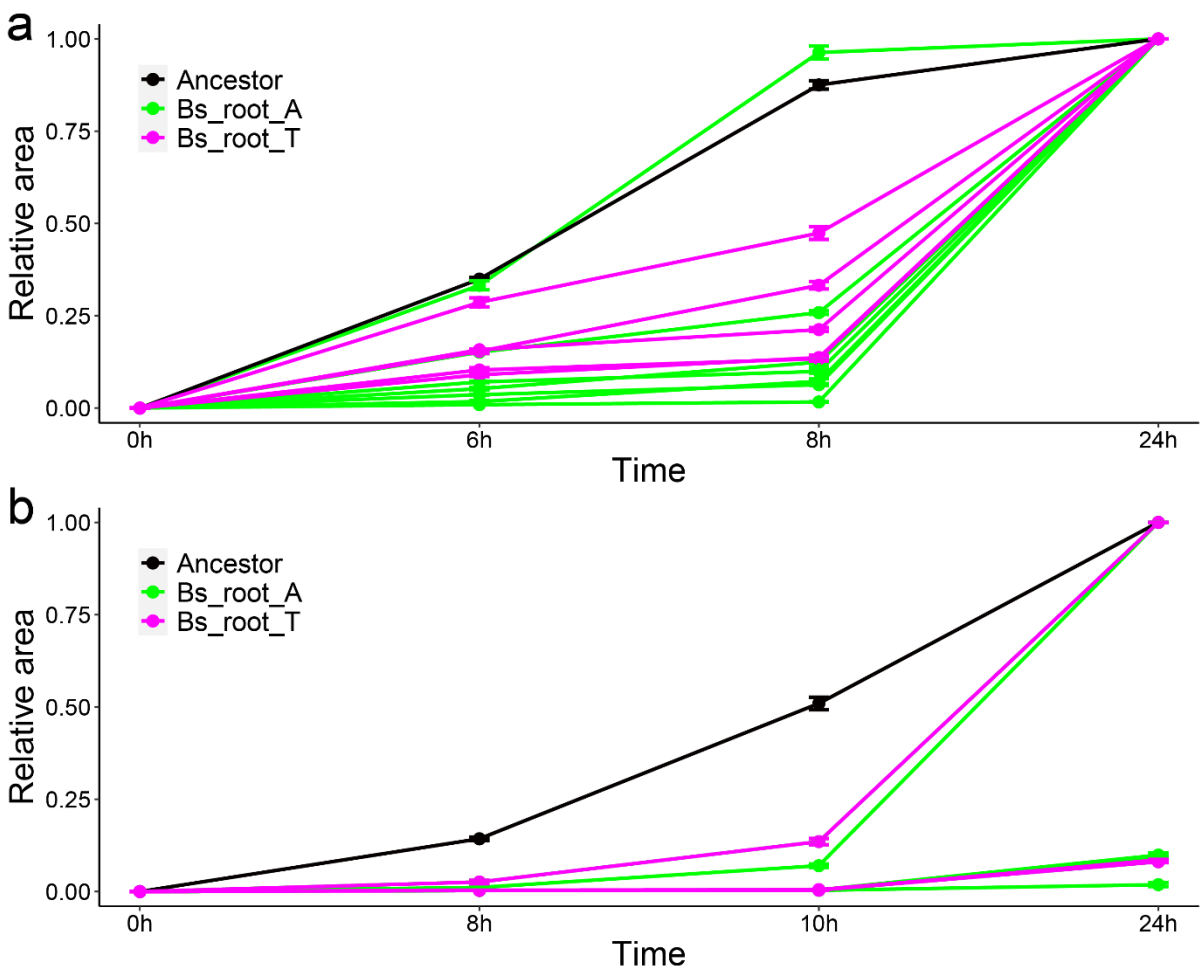

Fig. 2 Evolved isolates showed impaired motility. Swimming (a) and **Swarming (b)** motility of evolved isolates from Bs_root_A (green, 7 isolates) and Bs_root_T (magenta, 5 isolates) in comparison to the ancestor (**Black**). Notably, swarming motility of several isolates are similar and low, thus indistinguishable from each other in panel b. Data represent mean and error bars represent standard error, each isolate repeated for 3 times, the ancestor repeated for 9 times. Tested isolates include two SN from lineage A and E of Bs_root_A, two SM from lineage A and E of Bs_root_A, three WR from lineage A, D and E of Bs_root_A, and five WR from lineage A (1), B (2) and C (2) of Bs_root_T, respectively.

150 ***Mutation spectrum and genetic diversity***

151 Mutations provide the ultimate source of diversity, allowing selection to act and evolution to
152 take place. To understand the genetic basis behind the observed phenotypic diversification,
153 impaired motility, and the dynamic landscape of evolution, we employed a longitudinal whole-
154 population genome sequencing approach of 79 *B. subtilis* population samples (one population
155 sample was lost during freezer maintenance) and the ancestor strain, using the DNBSEQ-Tx
156 platform (Chen et al. 2022; Han et al. 2022). More than >200× coverage depth raw data were
157 generated for each sample. Mutation of SNPs, Indels (short insertions and deletions) were
158 detected compared with the ancestor, using *breseq* pipeline (version 0.35.7) (Barrick et al. 2014;
159 Deatherage & Barrick 2014). As default parameter, mutations were reported only if those
160 appeared at least two reads from each strand and reached a frequency of at least 5% in the
161 population. This analysis revealed 117, 106, 104, and 134 mutations in the evolved lineages
162 from the Bs_root_A, Bs_root_T, Bs_root_AT, and Bs_root_TA conditions (**Table 1**),
163 respectively. No significant difference in mutation numbers were detected between the
164 evolution conditions (Kruskal–Wallis test, p = 0.1277), though the mutation spectra were
165 slightly different between the selection setups (**Table 1**). When the filtering step excluded the
166 mutations below 10% frequency, the cyclic evolving conditions were found to contain more
167 mutations than the mono-evolved conditions (p = 0.0005162, t = -4.2419, df = 17.542 via two-
168 tailed t-test), suggesting that the mono-evolved conditions contained several low frequency
169 mutations, especially the Bs_root_A setup. Only 4 fixed mutations were present parallel in all
170 20 lineages, possibly due to the short transfer times used in the experiment.

171 **Table 1. mutation type and number**

Category	Bs_root_A	Bs_root_T	Bs_root_AT	Bs_root_TA
Pseudogene	0	1	0	0
Non-coding gene*	0	1	0	0
Coding gene	81	91	88	104
Synonymous	15	15	19	19
Non-synonymous	57	58	47	58
Nonsense	0	1	3	6
InDel**	9	17	19	21
Intergenic***	36	13	16	30
Total mutation number	117	106	104	134
Total mutation number (>10%)	50	69	80	92
Fixed	1	0	2	1

172 Notes: there is no overlap between each mutation type. * Non-coding gene includes tRNA
173 gene, ncRNA gene, and repeat region (IS); ** InDel indicates small insertions or deletions in
174 coding gene regions; *** Intergenic refers to all kinds of mutations occurred in intergenic
175 regions.

176

177 Though there was no significant difference in mutation numbers between the evolution
178 conditions, we expected that the population samples evolved in cyclic evolved conditions would

179 increase the genetic diversity compared with the mono-evolved conditions at the end of the
180 experiment due to the higher complexity and fluctuating nutrient composition caused by the
181 alternating host plants. Therefore, the genotype diversities of the endpoint samples were
182 compared between each condition. Indeed, the genotype diversity was significantly lower in
183 mono-evolved conditions than cyclic evolving conditions ($p = 0.01133$, t = -2.9044, df = 14.315
184 via two-tailed t-test), being lowest in Bs_root_A condition (**Fig. 3**).

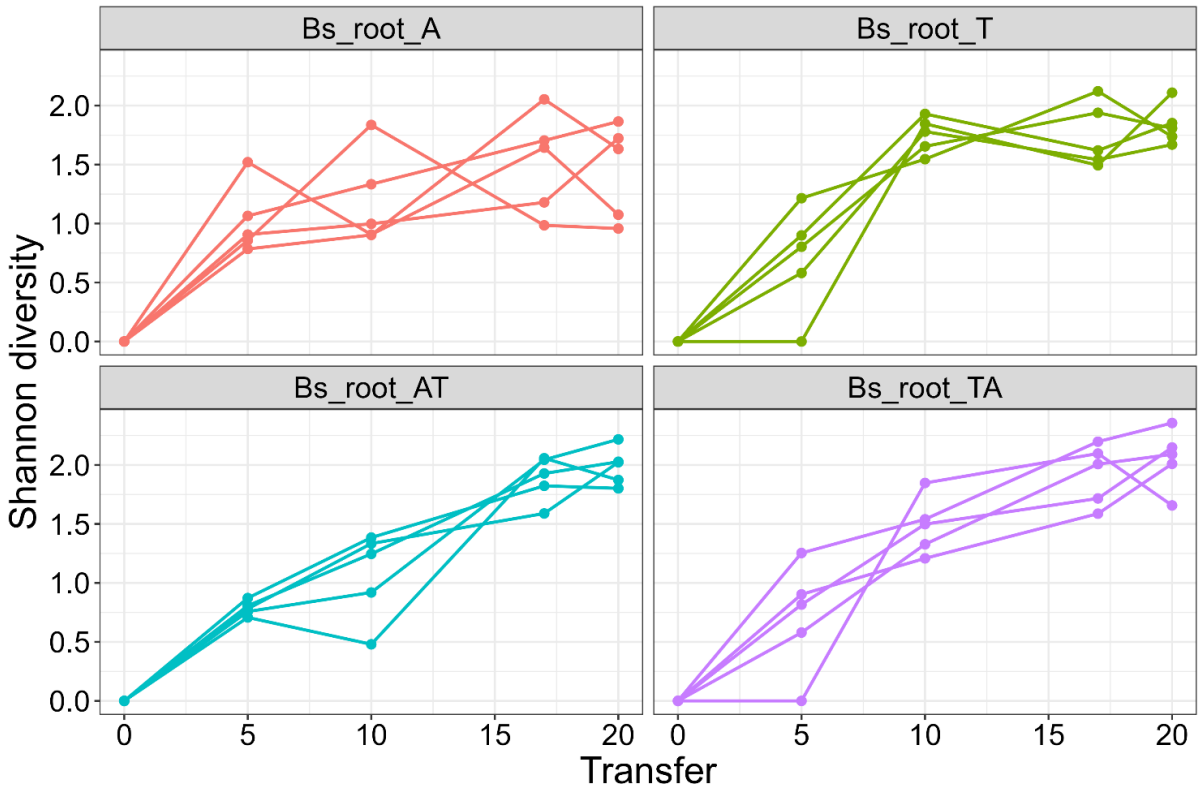

185

186 **Fig. 3 Genotype diversity.** Dynamic distribution of genotype alpha diversity (Shannon
187 method) in each population of four adaptation models over time. Genotype and their frequencies
188 were from genotype and genealogy analysis using *Lolipop*.

189

190 ***Ecological differentiation and parallel evolution***

191 To infer the ecological differentiation in each lineage and visualize the changes in lineage
192 frequencies from shared, nested mutation trajectories over time, we utilized the *Lolipop*
193 software package developed by Cooper and colleagues (Scribner et al. 2020; Harris et al. 2021).
194 An average of 16 ± 1.10, 15.6 ± 2.15, 14.6 ± 1.85, and 17.4 ± 2.15 genotypes were obtained in
195 Bs_root_A, Bs_root_T, Bs_root_AT, and Bs_root_TA conditions, respectively, with multiple
196 mutations in each genotype. Consistent with mutation number, there was no significant
197 difference in genotype numbers between evolved conditions (Kruskal–Wallis test, $p = 0.3129$).
198 Overall, the number of genotypes continuously increased in all conditions, consistently with
199 the detected genotype diversity in each condition. Notably, the genotype number or diversity
200 didn't reach a peak within the time frame of the experiment (**Fig. 3**).

201 Each of the lineage was dominated by a few genotypes which contain one or more
202 mutations in certain genes. In general, *sinR*, *pstBA*, *yuxH*, *sigD* and eight flagellum-related
203 genes were the most selected, demonstrating a high parallel evolution in gene and function-
204 level within and between different evolved conditions (**Fig. 4**). Diverse functional genes were
205 mutated, among which, the bacterial motility related genes were targeted most frequently,
206 which show high parallelism in functional level across all environments. To further compare
207 the genetic similarity between conditions, we determined the Jaccard Index (*J*) of all pairs of
208 lineages within each condition. The Jaccard Index is commonly used in measuring similarity,
209 indicating how likely it is for the same gene to be mutated in two separate lineages (Bailey et
210 al. 2015, 2017), ranging from 0 to 1. Again, we observed relatively lower genetic similarity in
211 mono-evolved conditions than that of cyclic evolved conditions, and lowest genetic similarity

212 within condition in the Bs_root_A, in which is significantly lower than that in Bs_root_T (p =
213 0.0249, t = -2.4471, df = 17.998 via two-tailed t-test) and the other two cyclic evolved
214 conditions ($p < 0.001$ and < 0.05, respectively) (**Fig. 5**).

215 Subsequently, we compared the genetic similarity between different evolved conditions.
216 The similarity between the two cyclic evolved conditions was much higher than the two mono-
217 evolved conditions (p = 2.628e-12, t = -10.022, df = 38.695 via two-tailed t-test), and the
218 similarity between Bs_root_A and two cyclic conditions were also much lower than the
219 similarity between Bs_root_T and two cyclic conditions (**Fig. 5**). These results strongly
220 indicated that the selection pressure imposed by the *A. thaliana* was much weaker than observed
221 with tomato, and the tomato root was potentially the main selective factor in the two cyclic
222 evolution conditions.

223 We observed high parallelism from root colonization ability and morphotype, to functional
224 pathway and gene level, additionally, extensive parallelism at the level of individual nucleotides
225 was also observed (**Supplementary Dataset 1**). One of the most striking examples, 18 out of
226 the 20 lineages contained a frameshift in gene *flhB*, which is required for flagellum and
227 nanotube assembly (Kuhlen et al. 2020). Another 8bp deletion found in gene *yuxH*, which is
228 involved in c-di-GMP regulation in *B. subtilis* (Chen, et al. 2012; Gao et al. 2013), was detected
229 in 15 lineages. Additional high parallelism mutations at nucleotide level, which occurred in
230 more than 10 lineages and belong to nonsynonymous mutations, occurred in *hag* and *sigD* genes.
231 Notably, all mutations mentioned above reach high frequency from 12.9% to 68.53% in the
232 evolution conditions.

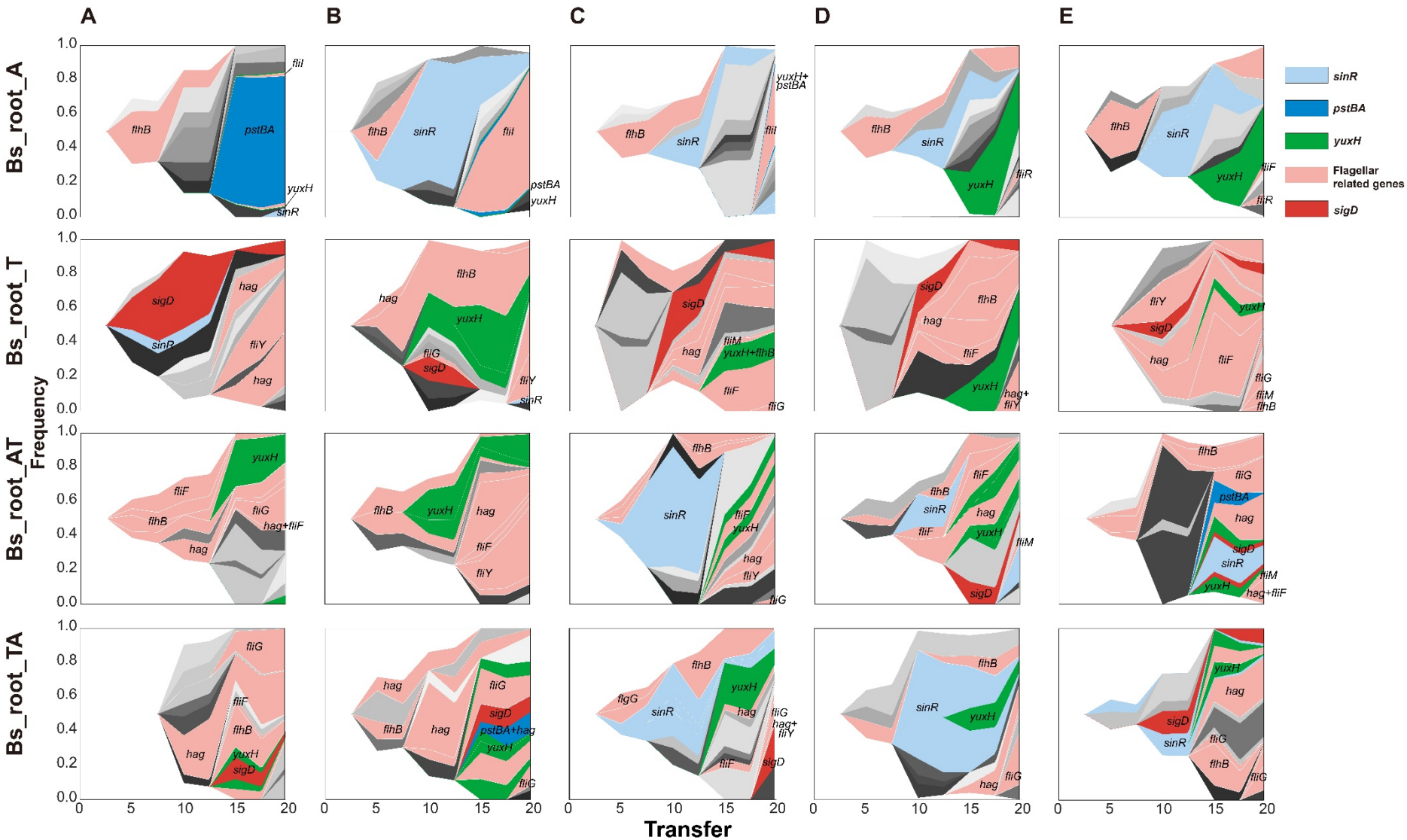
A
B
C
D
E
Bs_root_A
Bs_root_T
Bs_root_AT
Bs_root_TA
Frequency
Transfer
sinR
pstBA
yuxH
Flagellar related genes
sigD

233

234 **Fig. 4 Evolutionary dynamics of *B. subtilis* during plant root colonization.** Each shade or color represents a different genotype and vertical
235 area corresponds to genotype frequency, inferred by *Lolipop*. Genotypes under selective pressure in certain condition(s) are highlighted in different
236 colors and with annotates within or near the shadows, while the other genotypes are in different levels of gray without annotation. The nested
237 genotypes of the highlighted genotype are highlighted with the same color, except for the nested genotypes which also contain the genes under
238 selective pressure. Notably, some genotypes are less presented in the figure due to their frequencies are similar to their nested genotypes, like *fliI*
239 and *yuxH* in lineage A of Bs_root_A, *pstBA* and *yuxH* in lineage B and C of Bs_root_A. Different colors represent different genotypes contain
240 certain targeted genes, flagellar related genes include *fliF*, *fliI*, *fliR*, *flhB*, *fliG*, *fliM*, *fliY*, and *hag*. Genotypes containing more than one targeted
241 gene are colored with the color of the gene displayed in the front.

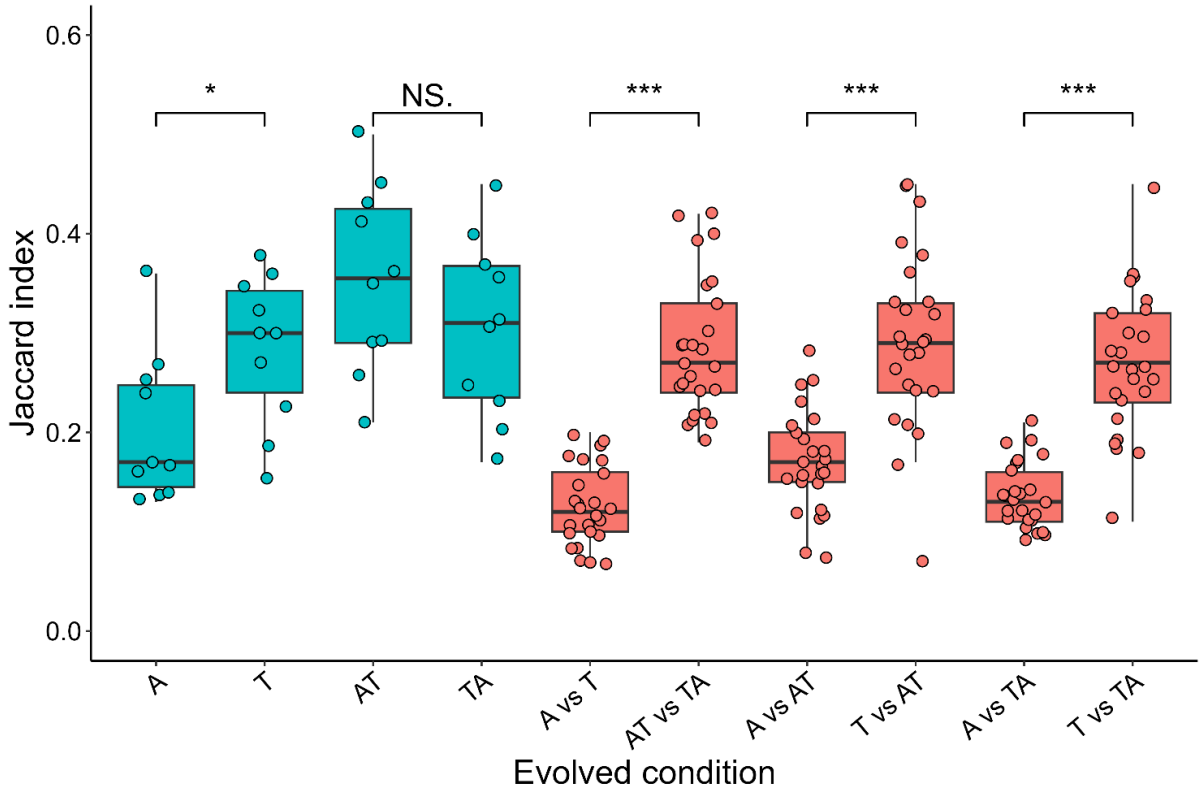

Fig. 5 Parallelism. Degree of parallelism within and between each evolved environment was estimated using the Jaccard index. Asterisks at the top indicate significant differences between different environment combinations (*$p < 0.05$, ***$p < 0.001$, by student's unpaired two-tailed t-test). Boxes indicate Q1–Q3, lines indicate the median, circles indicate the *J* value of each pair within (blue) or between (soft red) evolved conditions.

B. subtilis adapt specifically towards the plant species

The lower mutation number (frequency >10%), lower genotype diversity, and lower genetic similarity of Bs_root_A strongly imply that the adaptation strategy between Bs_root_A and other three conditions were different. Therefore, we focused on the genes with a mutation frequency higher than 10% and categorized them based on KEGG pathway. Overall, bacterial

254 motility proteins, genetic information processing and metabolism related genes were mutated
255 more frequently and reached high frequencies, account for 61.36% mutated genes
256 (frequency >10%).

257 As mentioned above, bacterial motility proteins were the most selected in our experiment.
258 Among the revealed motility protein genes, eight out of the eleven bacterial motility protein
259 genes are flagellar structure protein coding genes (**Fig. 6**) (Mukherjee & Kearns 2014), and
260 could be categorized into filament coding genes (flagellin, *hag*), basal body coding genes (*fliF*,
261 *fliG*, *fliM*, and *fliY*), and flagellar type III secretion (T3S) apparatus protein genes (*fliI*, *fliR*, and
262 *flhB*) (Mukherjee & Kearns 2014). Although bacterial motility genes were targeted frequently
263 in all conditions, *fliI* and *fliR* were only mutated in Bs_root_A and mutations in *fliG*, *fliY* and
264 *hag* were only absent in Bs_root_A. FliI is a flagellar-specific ATPase for the export of flagellar
265 proteins (Ibuki et al. 2011), and FliR is the part of the T3S apparatus (Kuhlen et al. 2018), which
266 required for flagellum and nanotube assembly. Another gene required for flagellum and
267 nanotube assembly, *flhB* (Kuhlen et al. 2020), was mutated in all evolved conditions. FliG
268 involved directly in flagellar rotation(Ward et al. 2019), while FliY interacts with the
269 chemotaxis system and control the direction of flagellar rotation (Sircar et al. 2013; Mukherjee
270 & Kearns 2014), and *hag* encoding the flagellin monomer protein Hag, which is also essential
271 for flagellar assembly (LaVallie & Stahl 1989; Hölscher et al. 2018). A sigma factor encoding
272 gene, *sigD*, which regulates flagella, motility, chemotaxis and autolysis in *B. subtilis* (Marquez
273 et al. 1990; Hölscher et al. 2015, 2018), was solely not mutated in the Bs_root_A samples, while
274 gene *yuxH* (*pdeH*), encoding for c-di-GMP degrading phosphodiesterase, was mutated in all

275 conditions and relatively high frequencies. c-di-GMP is a second messenger that regulates
276 diverse cellular processes in bacteria, including bacterial motility, biofilm formation, cell-cell
277 signaling, and host colonization (Chen, et al. 2012; Gao et al. 2013). Overall, species-specific
278 and common mutations in both flagellar structure proteins and motility regulator proteins were
279 identified, which were possibly caused by the species-specific evolution stress imposed by
280 different plant species and the same static hydroponic setup.

281 Mutation in a relevant gene for biofilm development, *sinR*, which codes for a DNA-binding
282 protein that regulate the expression of the operons involved in matrix production, *epsA-O* and
283 *tapA-sipW-tasA* (Kearns 2010; Chu et al. 2006), was only detected transiently with low
284 frequency (max at 7.19%) in Bs_root_T (**Fig. 4**, **Fig. 6** and **Supplementary Dataset 2**), while
285 it was observed more frequently and with higher frequency in the other conditions, suggesting
286 an *A. thaliana* specific mutation.

287 Another suspected *A. thaliana* specific mutated gene, *pstBA*, which encoding phosphate
288 transport system ATP-binding protein, was only absent in the Bs_root_T sample, and transiently
289 with low frequency in two cyclic evolved condition, while detected at high frequency in three
290 out of five lineages in Bs_root_A. *pstBA* belongs to the five genes containing *pst* operon, a
291 member of the PhoP-PhoR two-component signal transduction system (Atalla & Schumann
292 2003; Allenby et al. 2004; Moreno-Letelier et al. 2011). The encoded proteins are responsible
293 for phosphate uptake under nutrient stress in *B. subtilis* (Moreno-Letelier et al. 2011), while the
294 *pst* operon is alkali inducible (Atalla & Schumann 2003).

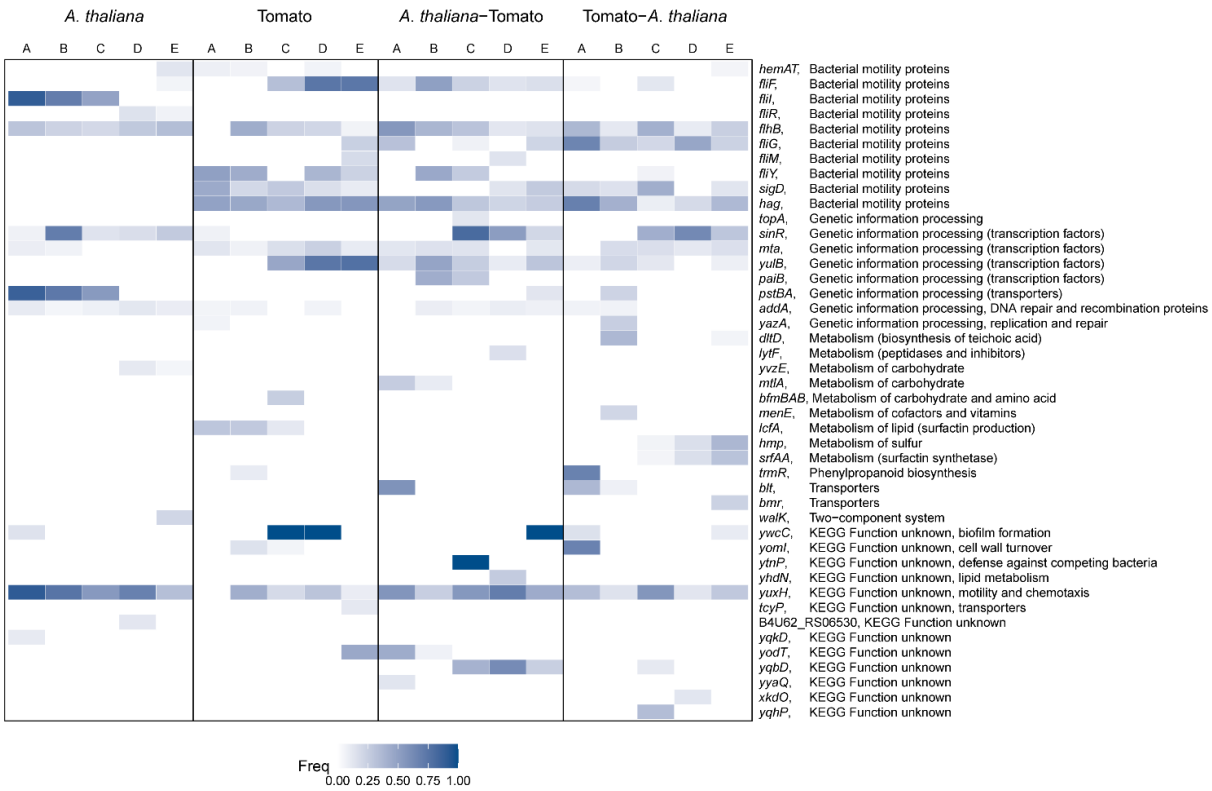

295

296 **Fig. 6 Genes with mutation frequency > 10%.** Each column represents one replicate

297 lineage. In each lineage, the color represents the highest frequency of mutations in that certain

298 gene. Detailed information of these genes and mutations can be found in **Supplementary**

299 **Dataset 2**.

300

301 # Discussion

302 Do plant colonizing bacteria adapt differently in an alternating host regime in comparison with
303 using the same plant throughout the experiment? Does a bacterial species adapt differently to
304 different plant hosts? To explore these questions, experimental evolution and whole-population
305 WGS sequencing method were exploited to analyze how *B. subtilis* evolves on *A. thaliana* and
306 tomato seedlings, as well as when these two plant hosts were alternating in a static hydroponic
307 setup (Blake, Nordgaard, et al. 2021). The observed data does not offer a simple binary answer
308 for the initial questions.

309 Similar to several previous studies (Blake, et al. 2021; Lin et al. 2021; Nordgaard et al.
310 2022), *B. subtilis* showed rapid improvement on root colonization ability, albeit at varying rates,
311 and diversified to three distinct morphotypes during adaptation in all evolved lineages and
312 conditions. Additionally, the three distinct morphotypes coexisted until the end of the evolution
313 experiment, reaching on average highly similar ratios in all four evolution experiments. Both
314 the root colonization improvement and morphotypic diversification displayed remarkable
315 degree of parallelism across all evolved conditions. Furthermore, all but one randomly selected
316 isolate from Bs_root_A and Bs_root_T showed impaired swimming and swarming motility.
317 The populations from two host-cyclic evolved conditions share numerous mutated genes with
318 Bs_root_T suggesting similar trade-offs being present in the alternating plant setup also.
319 Analysis of the genetic basis behind the two levels of parallelism (morphotypes and altered
320 motility) revealed bacterial motility proteins, genetic information processing, and metabolism
321 related genes to be mutated more frequently and reaching high frequencies in all evolved

322 conditions. Besides the parallelism on phenotypic and functional level, mutational resemblance
323 was observed in certain genes and even at individual nucleotide level. Two genes, *flhB* and
324 *yuxH*, showed striking parallelism on both gene and at individual nucleotide level, 18 out of the
325 20 lineages contained a frameshift in gene *flhB* and 15 lineages contained an 8bp deletion in
326 *yuxH*. *flhB* is required for flagellum and nanotube assembly and *yuxH* is involved in c-di-GMP
327 regulation in *B. subtilis* (Chen, et al. 2012; Gao et al. 2013), both may contribute to the
328 adaptation of *B. subtilis* to the plant roots related to motility. However, reintroduction of single
329 mutations alone or in combination will be necessary in the future to precisely measure the
330 influence of these mutations on fitness. Hereto, we identified repeated changes across multiple
331 levels of biological organization from phenotypic, functional pathways, genes, and even to
332 individual nucleotide (Bailey et al. 2015), demonstrating the overlapping strategies employed
333 by *B. subtilis* when adapting to *A. thaliana* and tomato roots as well as roots in an alternating
334 regime.

335 The static hydroponic setup used in our study selects for a regular root recolonization by
336 the bacterial cells on different plant species, that includes bacterial traits of chemotaxis, biofilm
337 formation and dispersal (Blake, et al. 2021). Different histidine kinases influence the
338 phosphorylation level of the global regulator, Spo0A (Jiang et al. 2000) when *B. subtilis* forms
339 a biofilm on the roots of *A. thaliana* (Chen, Cao, et al. 2012) and tomato (Beauregard et al.
340 2013), and different Bacillus species have distinct host plant colonization (Zhang et al. 2014).
341 These previous results motivated the hypothesis that *B. subtilis* adaptation to *A. thaliana* or
342 tomato will display distinct gene-level attributes behind the species-specific adaptation.

343 Although parallelism was identified at phenotypic and nucleotide change levels, obvious
344 differences were detected in the number of mutation (at a frequency >10%), the genotype
345 diversity, the mutated gene, and the genetic similarity between and among the different
346 conditions.

347 Less mutations (at a frequency >10%), lower genotype diversity, and lower within
348 condition genetic similarity were observed in mono-evolved conditions, especially in
349 Bs_root_A. The difference between mono-evolved condition and cyclic evolved conditions
350 could be explained by a more heterogeneous, multi-resource spatially structured environment
351 created by the host-cycling environment, suggesting that environmental heterogeneity might
352 have an important influence on adaptation (Bailey et al. 2015; Bram Van den Berghet al. 2018;
353 Harris et al. 2021). When *Pseudomonas fluorescens* is evolved in five different environments
354 that varied in resource type and arrangement, higher number of mutations and higher degree of
355 parallelism can be observed at gene level in the most heterogeneous environment (Bailey et al.
356 2015). Similarly, evolution of *Pseudomonas aeruginosa* populations on plastic beads that favors
357 a biofilm lifestyle exhibits higher morphologic diversity and mutation rates compared with
358 planktonic cultures (Flynn et al. 2016). Consistent with previous studies, the degree of parallel
359 evolution was significantly higher in the here described *B. subtilis* populations evolved in a
360 heterogeneous, multi-resource spatially structured environment.

361 Bs_root_A populations harbored the lowest number of mutations and the least similarity
362 among these, even lower than that of the Bs_root_T samples. Additionally, the genetic
363 similarity between the two mono-evolved conditions was much lower than between the two

364 cyclic evolved conditions, and the similarity between Bs_root_A and the two cyclic conditions
365 were also much lower than the similarity between Bs_root_T and the two cyclic conditions.
366 Furthermore, several specific mutated genes were also observed, which were present or absent
367 exclusively in one of the plant species. These results imply that the adaptation pattern of *B.*
368 *subtilis* to the root of *A. thaliana* and tomato was different, and *A. thaliana* exerted less influence
369 on the adaptation process in the two cyclic evolved conditions. A potential key difference
370 between *A. thaliana* and tomato that might alter bacterial evolution is the composition and
371 amounts of exudates. In our experimental system, *B. subtilis* was evolved in a minimal salt
372 medium (MSM; see **Materials and Methods**), where bacterial cells are dependent on carbon
373 sources provided by the plant for their growth. The composition and amount of exudates in and
374 between *A. thaliana* (Chaparro et al. 2013) and tomato (Kravchenko et al. 2003) plants varies
375 depending on the growth stage.

376 We found the most targeted genes to be related to motility, while all lineages displayed
377 improved root colonization. Motility and biofilm formation are considered to be inversely
378 regulated lifestyles with bacteria expressing genes necessary for either motility or biofilm
379 matrix production but not both simultaneously (Guttenplan & Kearns 2013; van Ditmarsch et
380 al. 2013). Motility is vital for many bacteria, as this process enables them to explore resources
381 and supports the dispersal of progeny (Wadhwa & Berg 2022). Motility has been shown to be
382 important for the effective root colonization of different plant species by *B subtilis* under
383 different conditions (Allard-Massicotte et al. 2016; Gao et al. 2016; Zhang et al. 2014; Tian et
384 al. 2021). It is not surprising that the loss of motility is repeatedly evolved in populations

385 growing in well-mixed liquid media where motility is not essential (Bailey et al. 2015) and
386 where the production of proteins for motility, primarily for flagella, is energy and resources
387 costly (Keegstra et al. 2022). A biofilm-motility trade-off was previous also suggested where *B.*
388 *subtilis* evolved on *A. thaliana* roots under shaking condition (Nordgaard et al. 2022).
389 Surprisingly, all mutations in flagellar structure protein coding genes were nonsynonymous
390 SNPs or InDels, suggesting these mutations to cause loss-of-function of flagella. Notably, a
391 78bp duplication (23 amino acids, 133~155) occurred in *hag* in three evolved conditions (in 12
392 lineages) and reached high frequency, which would strongly affect the structure and function
393 of flagellin, i.e. cell motility. Additionally, widespread and high frequency mutations in *sinR*,
394 which encoding biofilm master regulator (Kearns et al. 2005), *sigD*, encoding sigma factor D
395 (Marquez et al. 1990; Hölscher et al. 2015, 2018), which regulates flagella, motility, chemotaxis
396 and autolysis of *B. subtilis*, *yuxH*, which is involved in c-di-GMP regulation in *B. subtilis* (Chen,
397 Chai, et al. 2012; Gao et al. 2013), and *pstBA*, which responsible for phosphate uptake under
398 nutrient stress in *B. subtilis* (Moreno-Letelier et al. 2011), were all predicted to regulate the
399 motility-biofilm balance in *B. subtilis*.

400 Finally, we compared the genetic similarities and differences in certain biological functions,
401 e.g. aerotaxis, chemotaxis, motility (regulation) and biofilm development, when *B. subtilis* was
402 evolved under different experimental conditions, including a static air-medium pellicle biofilm
403 transfer mode (Bs_pellicle) (Dragoš et al. 2018), an *A. thaliana* root colonization study under
404 shaking hydroponic setup (Bs_root) (Nordgaard et al. 2022) and the here reported plant root
405 colonization under static hydroponic setup (Bs_root_ATTA) (**Supplementary Fig. 1**). Both

406 common and condition-specific genes were identified to carry mutations. We found *hemAT* to
407 be mutated in both Bs_pellicle and Bs_root_ATTA systems, although less frequently in
408 Bs_root_ATTA. Importantly, both experiments were performed under static condition, where
409 an oxygen gradient is generated in the culture and HemAT is a key oxygen sensor important
410 during pellicle formation (Hölscher et al. 2015). The lower frequency of mutation in *hemAT*
411 detected in Bs_root_ATTA suggests lower selection for aerotaxis in the cells that colonize the
412 submerged part of the plant roots compared with the cells that localized the medium-air
413 interface. Interestingly, the sigma factor encoding gene, *sigD*, was mutated only in conditions
414 where tomato was used as host in Bs_root_ATTA, suggesting that it is a tomato-specific
415 mutational target gene. Flagella related genes were identified to be mutated in all three
416 conditions, although mutations were detected in different genes and with different frequency.
417 Further, the c-di-GMP degrading phosphodiesterase-encoding *pdeH* was mutated in all three
418 conditions and more frequently and with high frequencies in Bs_root_ATTA. c-di-GMP is a
419 second messenger that modulates diverse cellular activities in bacteria, including bacterial
420 motility, biofilm formation, cell-cell signaling, and host colonization (Chen, et al. 2012; Gao et
421 al. 2013), however, studies c-di-GMP signaling have mostly focused on Gram-negative bacteria
422 until recently. *sinR*, seems to be a target in plant specific conditions as it solely lacked mutations
423 in the Bs_pellicle samples. Another possible static condition specific target similar to *hemAT* is
424 *pstBA*, which involved in high-affinity phosphate uptake in *B. subtilis* (Moreno-Letelier et al.
425 2011).

426 In conclusion, our study identified parallel evolution across multiple levels of biological

organization from phenotypic to individual nucleotide level, while the degree of parallel evolution in gene level was significantly higher in populations evolved in a heterogeneous, multi-resource spatially structured environment. We also observed species-specific adaptation at genetic level, which was possibly caused by the selection stress imposed by different host plants. Additionally, a strong trade-off between motility and growth as well as biofilm formation was observed under the here applied static selection condition. Finally, we identified several condition-specific and common mutated genes by comparing the genetic similarities and differences between three studies.

435 # Materials and Methods

436 **Bacterial strains and experimental methods**

437 We used identical materials and methods for the tomato and two host-cycling evolution setups
438 as described in detail previously for the *A. thaliana* selection approach (Blake, et al. 2021),
439 including the bacterial strain and the culture conditions, the seedling preparation, the
440 experimental evolution, and the morphological diversification experiments.

441 **Motility assays**

442 20 mL of either 0.3% or 0.7% lysogeny broth (LB)-agar plates were used to test swimming and
443 swarming motility. In both cases, the plates were dried for exactly 20 minutes before the
444 bacterial cultures were applied to the center of the plates. 2 µL overnight cultures of the ancestor
445 or evolved isolates adjusted to an OD_{600} of 5.0 were spotted in the middle of the plate. To keep
446 a similar humidity across all plates, multiple stacking was avoided. Plates were incubated at
447 30°C and images were taken for swimming after 6h, 8h and 24h and for swarming after 8h, 10h
448 and 24h with a camera (Lumix DC T290, Panasonic equipped with lens DC Vario-ELMAR,
449 Leica). The area the bacterial cells covered at a given time point as well as the area of the whole
450 agar plate were measured using ImageJ (Fiji ImageJ 1.52p). The capacity in swimming and
451 swarming motility was calculated by dividing the covered area by the total area.

452 **Sequencing and variant calling**

453 Archived samples from each experimental evolution environment were revived via cultivation
454 in lysogeny broth (LB; Lennox, Carl Roth; 10 g/L tryptone, 5 g/L yeast extract, and 5 g/L NaCl)

455 medium at 37℃ for 16 hours. Then the genomic DNA was extracted from the harvested cells
456 from each culture using EURx Bacterial and Yeast Genomic DNA kit.

457 For whole-population genome sequencing of the evolved populations and ancestor strain
458 samples, the MGIEasy PCR-free Library Prep Set (MGI Tech) was used for libraries
459 preparation. 150bp × 2 pair-end sequencing were performed on a DNBSEQ-Tx sequencer (MGI
460 Tech) following the manufacturer's procedures(Chen et al. 2022; Han et al. 2022). More than
461 200× depth coverage raw data were generated for All population samples for further
462 polymorphism calling.

463 To remove low quality data, filtering was performed using SOAPnuke (version 1.5.6)
464 (Chen et al. 2018). Therefore, reads including more than 50% of bases with quality lower than
465 12, reads including more than 10% of unknown base "N", and reads containing adaptor
466 contamination were removed. Subsequently, the derived data was normalized to 200× depth for
467 all sample to ensure a similar variants calling sensitivity. Mutations were reported by using
468 *breseq* (version 0.35.7) with the default parameters and a -p option for population samples
469 (Deatherage & Barrick 2014; Barrick et al. 2014). The default parameters reported mutations
470 only if they appeared at least two reads from each strand and reached a frequency of at least 5%
471 in the population. Mutations that also found in the ancestor strains were removed for further
472 analysis.

473 **Genotype inferences from populations and Muller plots**

474 To generate the muller plots, the *Lolipop* package (https://github.com/cdeitrick/lolipop)

475 (version 0.6) was used with default parameters (Scribner et al. 2020; Harris et al. 2021). These
476 methods predict genotypes and lineages based on the shared trajectories of mutations over time
477 test their probability of nonrandom genetic linkage. Muller plots were then manually colored
478 by the presence of shared mutated genes or genotypes. The genotypes and their frequencies
479 were used for genotype diversity calculation in R (version 4.2.2) with the package vegan
480 (version 2.6-4).

481 **Jaccard Index calculation**

482 Jaccard Index (*J*) for two evolved lineages was calculated using formula (1), given two
483 lineage, each contains mutated gene set G1 and G2, respectively. In words, *J* is the number of
484 genes mutated genes in both lineages divided by the total number of genes mutated in both
485 lineages. *J* ranges from 0 to 1, with 1 indicating two lineages have exactly the same set of
486 mutated genes and 0 indicating no mutated genes in two lineages are shared. This value was
487 calculated for all pairs of evolved lineages, both within and between evolved environments.

488 $$J_{G1,G2} = \frac{|G1 \cap G2|}{|G1 \cup G2|} \quad (1)$$

489 **Data availability**

490 The sequencing data underlying this article are available in CNGB Sequence Archive (CNSA)
491 (Guo et al. 2020) of China National GeneBank DataBase (CNGBdb) (Chen et al. 2020) with
492 accession number CNP0002416 and CNP0003952. Note, the ancestor DK1042 strain data are
493 available in project CNP0002416.

494 **Acknowledgements**

This project was supported by China National GeneBank (CNGB), Danish National Research Foundation (DNRF137) for the Center for Microbial Secondary Metabolites, and Novo Nordisk Foundation within the INTERACT project of the Collaborative Crop Resiliency Program (NNF19SA0059360).

500 # Reference

501 Allard-Massicotte R et al. 2016. *Bacillus subtilis* Early Colonization of *Arabidopsis thaliana*
502 Roots involves multiple chemotaxis receptors Straight, PD & Ruby, EG, editors. mBio.
503 7:e01664-16. doi: 10.1128/mBio.01664-16.

504 Allenby NEE et al. 2004. Post-transcriptional regulation of the *Bacillus subtilis pst* operon
505 encoding a phosphate-specific ABC transporter. Microbiology (N Y). 150:2619–2628. doi:
506 10.1099/mic.0.27126-0.

507 Arnaouteli S, Bamford NC, Stanley-Wall NR, Kovács ÁT. 2021. *Bacillus subtilis* biofilm
508 formation and social interactions. Nat Rev Microbiol. 19:600–614. doi: 10.1038/s41579-021-
509 00540-9.

510 Atalla A, Schumann W. 2003. The *pst* Operon of *Bacillus subtilis* Is Specifically Induced by
511 Alkali Stress. J Bacteriol. 185:5019–5022. doi: 10.1128/JB.185.16.5019-
512 5022.2003/ASSET/F2AE8CF0-4236-48BF-8557-
513 B0E383D6314C/ASSETS/GRAPHIC/JB1630029006.JPEG.

514 Badri D v., Weir TL, van der Lelie D, Vivanco JM. 2009. Rhizosphere chemical dialogues:
515 plant–microbe interactions. Curr Opin Biotechnol. 20:642–650. doi:
516 10.1016/J.COPBIO.2009.09.014.

517 Bailey SF, Blanquart F, Bataillon T, Kassen R. 2017. What drives parallel evolution?: How
518 population size and mutational variation contribute to repeated evolution. BioEssays.
519 39:1600176. doi: 10.1002/BIES.201600176.

520 Bailey SF, Rodrigue N, Kassen R. 2015. The Effect of Selection Environment on the Probability
521 of Parallel Evolution. Mol Biol Evol. 32:1436–1448. doi: 10.1093/MOLBEV/MSV033.

522 Barrick JE et al. 2014. Identifying structural variation in haploid microbial genomes from short-
523 read resequencing data using *breseq*. BMC Genomics. 15:1039. doi: 10.1186/1471-2164-15-
524 1039.

525 Beauregard PB, Chai Y, Vlamakis H, Losick R, Kolter R. 2013. *Bacillus subtilis* biofilm
526 induction by plant polysaccharides. Proc Natl Acad Sci U S A. 110:1621–1630. doi:
527 10.1073/pnas.1218984110.

528 Blake C, Christensen MN, Kovács ÁT. 2021. Molecular Aspects of Plant Growth Promotion
529 and Protection by *Bacillus subtilis*. Molecular Plant-Microbe Interactions. 34:15–25. doi:

530 10.1094/MPMI-08-20-0225-CR.

531 Blake C, Nordgaard M, Maróti G, Kovács ÁT. 2021. Diversification of *Bacillus subtilis* during
532 experimental evolution on *Arabidopsis thaliana* and the complementarity in root colonization
533 of evolved subpopulations. Environ Microbiol. 23:6122–6136. doi: 10.1111/1462-2920.15680.

534 Bram Van den Bergh, Toon Swings, Maarten Fauvart JM. 2018. Experimental Design,
535 Population Dynamics, and Diversity in Microbial Experimental Evolution. Microbiology and
536 Molecular Biology Reviews. 82:e00008-18. doi: https://doi.org/10.1128/MMBR .00008-18.

537 Chaparro JM et al. 2013. Root Exudation of Phytochemicals in Arabidopsis Follows Specific
538 Patterns That Are Developmentally Programmed and Correlate with Soil Microbial Functions
539 Wu, K, editor. PLoS One. 8:e55731. doi: 10.1371/journal.pone.0055731.

540 Chen A et al. 2022. Spatiotemporal transcriptomic atlas of mouse organogenesis using DNA
541 nanoball-patterned arrays. Cell. 185:1777-1792.e21. doi: 10.1016/j.cell.2022.04.003.

542 Chen FZ et al. 2020. CNGBdb: China National GeneBank DataBase. Hereditas. 42:799–809.
543 doi: 10.16288/j.yczz.20-080.

544 Chen Y, Cao S, et al. 2012. A *Bacillus subtilis* sensor kinase involved in triggering biofilm
545 formation on the roots of tomato plants. Mol Microbiol. 85:418–430. doi: 10.1111/j.1365-
546 2958.2012.08109.x.

547 Chen Y, Chai Y, Guo J-H, Losick R. 2012. Evidence for Cyclic Di-GMP-Mediated Signaling
548 in *Bacillus subtilis*. J Bacteriol. 194:5080–5090. doi: 10.1128/JB.01092-12.

549 Chen Yuxin et al. 2018. SOAPnuke: A MapReduce acceleration-supported software for
550 integrated quality control and preprocessing of high-throughput sequencing data. Gigascience.
551 7:gix120. doi: 10.1093/gigascience/gix120.

552 Chu F, Kearns DB, Branda SS, Kolter R, Losick R. 2006. Targets of the master regulator of
553 biofilm formation in *Bacillus subtilis*. Mol Microbiol. 59:1216–1228. doi: 10.1111/J.1365-
554 2958.2005.05019.X.

555 Deatherage DE, Barrick JE. 2014. Identification of Mutations in Laboratory-Evolved Microbes
556 from Next-Generation Sequencing Data Using *breseq*. Methods Mol Biol. 1151:165–188. doi:
557 10.1007/978-1-4939-0554-6_12.

558 van Ditmarsch D et al. 2013. Convergent evolution of hyperswarming leads to impaired biofilm
559 formation in pathogenic bacteria. Cell Rep. 4:697–708. doi: 10.1016/j.celrep.2013.07.026.

560 Dragoš A et al. 2018. Evolution of exploitative interactions during diversification in *Bacillus*
561 *subtilis* biofilms. FEMS Microbiol Ecol. 94:fix155. doi: 10.1093/femsec/fix155.

562 Flynn KM et al. 2016. Evolution of ecological diversity in biofilms of *Pseudomonas aeruginosa*
563 by altered cyclic diguanylate signaling. J Bacteriol. 198:2608–2618. doi: 10.1128/JB.00048-16.

564 Gao S, Wu H, Yu X, Qian L, Gao X. 2016. Swarming motility plays the major role in migration
565 during tomato root colonization by *Bacillus subtilis* SWR01. Biological Control. 98:11–17. doi:
566 10.1016/j.biocontrol.2016.03.011.

567 Gao X et al. 2013. Functional Characterization of Core Components of the *Bacillus subtilis*
568 Cyclic-Di-GMP Signaling Pathway. J Bacteriol. 195:4782–4792. doi: 10.1128/JB.00373-13.

569 Guo X et al. 2020. CNSA: A data repository for archiving omics data. Database. 2020:baaa055.
570 doi: 10.1093/database/baaa055.

571 Guttenplan SB, Kearns DB. 2013. Regulation of flagellar motility during biofilm formation.
572 FEMS Microbiol Rev. 37:849–871. doi: 10.1111/1574-6976.12018.

573 Haichar F el Z, Heulin T, Guyonnet JP, Achouak W. 2016. Stable isotope probing of carbon
574 flow in the plant holobiont. Curr Opin Biotechnol. 41:9–13. doi:
575 10.1016/J.COPBIO.2016.02.023.

576 Hamon MA, Lazazzera BA. 2001. The sporulation transcription factor Spo0A is required for
577 biofilm development in *Bacillus subtilis*. Mol Microbiol. 42:1199–1209. doi: 10.1046/J.1365-
578 2958.2001.02709.X.

579 Han L et al. 2022. Cell transcriptomic atlas of the non-human primate *Macaca fascicularis*.
580 Nature. 604:723–731. doi: 10.1038/s41586-022-04587-3.

581 Harris KB, Flynn KM, Cooper VS. 2021. Polygenic Adaptation and Clonal Interference Enable
582 Sustained Diversity in Experimental Pseudomonas aeruginosa Populations. Mol Biol Evol.
583 38:5359–5375. doi: 10.1093/molbev/msab248.

584 Hölscher T et al. 2018. Impaired competence in flagellar mutants of *Bacillus subtilis* is
585 connected to the regulatory network governed by DegU. Environ Microbiol Rep. 10:23–32. doi:
586 10.1111/1758-2229.12601.

587 Hölscher T et al. 2015. Motility, Chemotaxis and Aerotaxis Contribute to Competitiveness
588 during Bacterial Pellicle Biofilm Development. J Mol Biol. 427:3695–3708. doi:
589 10.1016/j.jmb.2015.06.014.

590 Hölscher T, Kovács ÁT. 2017. Sliding on the surface: bacterial spreading without an active
591 motor. Environ Microbiol. 19:2537–2545. doi: 10.1111/1462-2920.13741.

592 Ibuki T et al. 2011. Common architecture of the flagellar type III protein export apparatus and
593 F- and V-type ATPases. Nat Struct Mol Biol. 18:277–282. doi: 10.1038/nsmb.1977.

594 Jiang M, Shao W, Perego M, Hoch JA. 2000. Multiple histidine kinases regulate entry into
595 stationary phase and sporulation in *Bacillus subtilis*. Mol Microbiol. 38:535–542. doi:
596 10.1046/J.1365-2958.2000.02148.X.

597 Kearns DB. 2010. A field guide to bacterial swarming motility. Nat Rev Microbiol. 8:634–644.
598 doi: 10.1038/nrmicro2405.

599 Kearns DB, Chu F, Branda SS, Kolter R, Losick R. 2005. A master regulator for biofilm
600 formation by *Bacillus subtilis*. Mol Microbiol. 55:739–749. doi: 10.1111/J.1365-
601 2958.2004.04440.X.

602 Keegstra JM, Carrara F, Stocker R. 2022. The ecological roles of bacterial chemotaxis. Nat Rev
603 Microbiol. 20:491–504. doi: 10.1038/s41579-022-00709-w.

604 Kovács ÁT, Grau R, Pollitt EJG. 2017. Surfing of bacterial droplets: *Bacillus subtilis* sliding
605 revisited. Proceedings of the National Academy of Sciences. 114:E8802. doi:
606 10.1073/pnas.1710371114.

607 Kravchenko L V. et al. 2003. Root exudates of tomato plants and their effect on the growth and
608 antifungal activity of *Pseudomonas* strains. Microbiology (N Y). 72:37–41. doi:
609 10.1023/A:1022269821379.

610 Kuhlen L et al. 2018. Structure of the Core of the Type Three Secretion System Export
611 Apparatus. Nat Struct Mol Biol. 25:583. doi: 10.1038/S41594-018-0086-9.

612 Kuhlen L et al. 2020. The substrate specificity switch FlhB assembles onto the export gate to
613 regulate type three secretion. Nat Commun. 11:1296. doi: 10.1038/s41467-020-15071-9.

614 Lareen A, Burton F, Schäfer P. 2016. Plant root-microbe communication in shaping root
615 microbiomes. Plant Mol Biol. 90:575–587. doi: 10.1007/S11103-015-0417-8.

616 LaVallie ER, Stahl ML. 1989. Cloning of the flagellin gene from *Bacillus subtilis* and
617 complementation studies of an in vitro-derived deletion mutation. J Bacteriol. 171:3085–3094.
618 doi: 10.1128/jb.171.6.3085-3094.1989.

619 Lenski RE. 2017. What is adaptation by natural selection? Perspectives of an experimental
620 microbiologist Doolittle, WF, editor. PLoS Genet. 13:e1006668. doi:
621 10.1371/journal.pgen.1006668.

622 Li Erqin et al. 2021. Experimental-evolution-driven identification of arabidopsis rhizosphere
623 competence genes in *Pseudomonas protegens*. mBio. 12:e00927-21. doi:
624 10.1128/MBIO.00927-21/SUPPL_FILE/MBIO.00927-21-SF005.JPG.

625 Li Minghui et al. 2021. Crop rotation history constrains soil biodiversity and multifunctionality
626 relationships. Agric Ecosyst Environ. 319:107550. doi: 10.1016/J.AGEE.2021.107550.

627 Lin Y et al. 2021. Adaptation of Bacillus thuringiensis to Plant Colonization Affects
628 Differentiation and Toxicity. mSystems. 6:e00864-21. doi: 10.1128/msystems.00864-21.

629 Marquez LM et al. 1990. Studies of σ(D)-dependent functions in *Bacillus subtilis*. J Bacteriol.
630 172:3435–3443. doi: 10.1128/jb.172.6.3435-3443.1990.

631 Moreno-Letelier A, Olmedo G, Eguiarte LE, Martinez-Castilla L, Souza V. 2011. Parallel
632 Evolution and Horizontal Gene Transfer of the *pst* Operon in Firmicutes from Oligotrophic
633 Environments. Int J Evol Biol. 2011:781642. doi: 10.4061/2011/781642.

634 Mukherjee S, Kearns DB. 2014. The structure and regulation of flagella in *Bacillus subtilis*.
635 Annu Rev Genet. 48:319–340. doi: 10.1146/annurev-genet-120213-092406.

636 Nordgaard M et al. 2022. Experimental evolution of *Bacillus subtilis* on *Arabidopsis thaliana*
637 roots reveals fast adaptation and improved root colonization. iScience. 25:104406. doi:
638 10.1016/j.isci.2022.104406.

639 Peng G et al. 2011. Potential biological control of clubroot on canola and crucifer vegetable
640 crops. Plant Pathol. 60:566–574. doi: 10.1111/J.1365-3059.2010.02400.X.

641 Sasse J, Martinoia E, Northen T. 2018. Feed Your Friends: Do Plant Exudates Shape the Root
642 Microbiome? Trends Plant Sci. 23:25–41. doi: 10.1016/j.tplants.2017.09.003.

643 Schmidt JE, Bowles TM, Gaudin ACM. 2016. Using ancient traits to convert soil health into
644 crop yield: Impact of selection on maize root and rhizosphere function. Front Plant Sci. 7:373.
645 doi: 10.3389/FPLS.2016.00373/BIBTEX.

646 Scribner MR et al. 2020. Parallel evolution of tobramycin resistance across species and
647 environments. mBio. 11:e00932-20. doi: 10.1128/mBio.00932-20.

648 Sircar R, Greenswag AR, Bilwes AM, Gonzalez-Bonet G, Crane BR. 2013. Structure and
649 activity of the flagellar rotor protein fliY: A member of the cheC phosphatase family. Journal
650 of Biological Chemistry. 288:13493–13502. doi: 10.1074/jbc.M112.445171.

651 Tian T et al. 2021. Sucrose triggers a novel signaling cascade promoting *Bacillus subtilis*
652 rhizosphere colonization. ISME J. 15:2723–2737. doi: 10.1038/s41396-021-00966-2.

653 Venturi V, Keel C. 2016. Signaling in the Rhizosphere. Trends Plant Sci. 21:187–198. doi:
654 10.1016/J.TPLANTS.2016.01.005.

655 Vives-Peris V, de Ollas C, Gómez-Cadenas A, Pérez-Clemente RM. 2020. Root exudates: from
656 plant to rhizosphere and beyond. Plant Cell Rep. 39:3–17. doi: 10.1007/s00299-019-02447-5.

657 Wadhwa N, Berg HC. 2022. Bacterial motility: machinery and mechanisms. Nat Rev Microbiol.
658 20:161–173. doi: 10.1038/s41579-021-00626-4.

659 Ward E et al. 2019. Organization of the flagellar switch complex of *Bacillus subtilis*. J Bacteriol.
660 201:e00626-18. doi: 10.1128/JB.00019-19.

661 Wei F, Hu X, Xu X. 2016. Dispersal of *Bacillus subtilis* and its effect on strawberry
662 phyllosphere microbiota under open field and protection conditions. Scientific Reports 2016
663 6:1. 6:1–9. doi: 10.1038/srep22611.

664 Zhang N et al. 2014. Effects of different plant root exudates and their organic acid components
665 on chemotaxis, biofilm formation and colonization by beneficial rhizosphere-associated
666 bacterial strains. Plant Soil. 374:689–700. doi: 10.1007/S11104-013-1915-6/FIGURES/6.

667